

RSC Advances



This is an *Accepted Manuscript*, which has been through the Royal Society of Chemistry peer review process and has been accepted for publication.

Accepted Manuscripts are published online shortly after acceptance, before technical editing, formatting and proof reading. Using this free service, authors can make their results available to the community, in citable form, before we publish the edited article. This *Accepted Manuscript* will be replaced by the edited, formatted and paginated article as soon as this is available.

You can find more information about *Accepted Manuscripts* in the [Information for Authors](#).

Please note that technical editing may introduce minor changes to the text and/or graphics, which may alter content. The journal's standard [Terms & Conditions](#) and the [Ethical guidelines](#) still apply. In no event shall the Royal Society of Chemistry be held responsible for any errors or omissions in this *Accepted Manuscript* or any consequences arising from the use of any information it contains.



Nitrogen-doped Carbon Dots as fluorescent probe for Detection of Curcumin Based on the Inner Filter Effect

Qingyan Zhang,^a Caihong Zhang,^a Zengbo Li,^a Jinyin Ge,^a Chenzhong Li,^a Chuan Dong^a and Shaomin Shuang^{a,*}

Received 00th January 20xx,
Accepted 00th January 20xx

DOI: 10.1039/x0xx00000x

www.rsc.org/

A facile, economical and green one-step hydrothermal method for N-doped CDs was presented by using citric acid as carbon source and urea as nitrogen source. The as-prepared N-doped CDs possess an average size of 5.23nm and exhibit high fluorescent quantum yield of 25.4%, good water solubility, and excellent photostability. The fluorescence of N-doped CDs may be quenched dramatically from curcumin via inner filter effect. The sensitive detection method of curcumin in aqueous solution was developed with the linear range of 2.0×10^{-7} - 1.0×10^{-5} mol/L and detection limit of 8.48×10^{-8} mol/L ($S/N=3$). The other common ions and related compounds could not interfere detection of curcumin with good selectivity. The proposed method was successfully applied to the determination of curcumin in urine samples and the recoveries were 95.71-103.81%.

1 Introduction

Curcumin (Fig. S1 †), a polyphenolic pigment derived from the root of the plant *Curcuma longa* L., is cultivated in some tropical parts of Asia^[1] and used as a common ingredient in spices, cosmetics and traditional Chinese medicine.^[2-5] It attracts considerable interest due to its biological and pharmacological activities including anti-inflammatory, anti-oxidant, anti-carcinogenic, anti-HIV etc.^[6] However, recent studies have demonstrated that excessive dose of curcumin treatment shows prooxidant activity on DNA^[7] as well as induces intracellular ATP levels to decrease and triggers necrosis processes^[8]. Therefore, the investigation on determination of curcumin with reliable, rapid and simple assay is essential for clinical medicine and pharmacology.

Numerous analytical assays for curcumin have been involved including spectrofluorometry,^[9-11] UV-vis spectrophotometry,^[12] Capillary Electrophoresis,^[13] Voltammetric,^[14] HPLC,^[15-17] and LC-MS^[18] and so on. Most of them were compromised by requiring expensive equipment and the time-consuming, complicated sample pretreatment. The fluorimetry took the fancy of the public because of its intrinsically high sensitivity, facile, rapid, and cost-effective advantages. However, the fact that fluorescence of curcumin decrease strongly in aqueous solution makes its determination difficult.^[9] Peinado et al.^[11] developed the direct and synchronous fluorimetric approach for the determination of curcumin in acetonitrile. Chen et al.^[19] constructed the resonance light

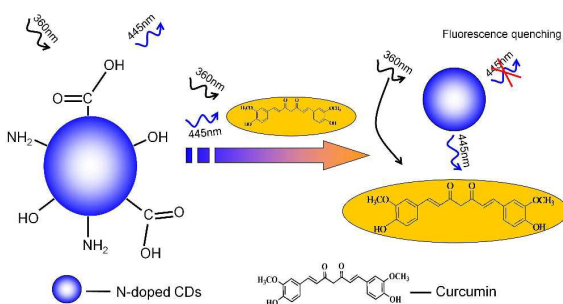
scattering assay for curcumin using Cu (II) ion as the spectral probe. Our previous research^[20] developed a reliable ratiometric fluorescent probe based on Mn-doped ZnS quantum dots with 3-Mercaptopropionic acid for monitoring of curcumin. However, the toxicity of 3-Mercaptopropionic acid is unavoidable in operation. We attempt to develop the alternative towards sensitive, facile and environmental friendly concept.

Carbon dots (CDs) emerged as a novel nanomaterial have attracted growing attention due to their excellent photostability, tunable excitation and emission spectra, low toxicity and favorable biocompatibility.^[21-23] In view of these exciting features, CDs have shown great potential in a variety of applications, especially in the aspects of photocatalysis, bioimaging and sensors.^[24-28] To date, tremendous effort has been spent on developing synthetic methods for various types of CDs. These approaches can be classified into two main categories: top-down and bottom-up methods. To achieve highly luminescent CDs, surface passivation reagents were usually required, and the reported quantum yields for CDs without surface passivation are relatively low (approximately 1%). Heteroatoms doping is an effective approach to tune the PL properties of CDs and doped CDs remain almost all the advantages of blank CDs and provide improved efficiency.^[29] N-doping is the current most popular way to enhance the emission of the CDs by inducing an upward shift in the Fermi level and electrons in the conduction band.^[30] Giannelis et al.^[31] reported pyrolysis of citric acid and ethanolamine at 230 °C to obtain N-doped CDs, which

^a Department of Chemistry and Chemical Engineering, Shanxi University, Taiyuan 030006, People's Republic of China. E-mail: smshuang@sxu.edu.cn; Fax: +86-351-7011688; Tel: +86-351-7018842

† Electronic supplementary information (ESI) available: chemical structures of curcumin, Hydrodynamic diameter distribution of CDs, the spectral overlap different pH values. Comparison of different methods for curcumin detection. HPLC method for determination of curcumin. See DOI: 10.1039/x0xx00000x

contributed to a dramatic increase in the PL enhancement. Based on the unique PL behaviour, N-doped CDs have been extensively explored as the platform for detection of ions,^[32-34] biomolecules and drugs. Zhao et al.^[35] synthesized N-doped CDs for label-free detection of Cu^{2+} / Fe^{3+} and cellular imaging. Lv et al.^[36] designed a sensitive probe for glutathione based on the fluorescence turn off and on of the CDs- Cu^{2+} system. Conventional sensing strategies for CDs like energy or electron transfer processes need the intermolecular connection of target molecule with CDs in a particular distance or geometry, making the method complicated and time-consuming. Inner filter effect (IFE) as the alternative is a necessary supplementary. The IFE is usually considered as an annoying source of errors in spectrofluorometry. However, it can be useful for an optical sensor in some cases by converting the analytical absorption signals into fluorescence signals without any covalent linking between the receptor and a fluorophore.^[37] Moreover, due to the conversion between the absorbance of sensors transform exponentially into fluorescence intensity changes, an enhanced sensitivity for this strategy is reasonable compared with the absorbance values alone.^[38] Sun et al.^[39] first introduced the Inner filter effect of CDs to fluorescent sensing system for recognition of Cr(VI), where Cr(VI) as an absorber to modulate the emission of the CDs. Inspired by this research, we try to develop CDs fluorescence assay with IFE behavior. Herein, we employed facile hydrothermal treatment to prepare N-doped CDs using citric acid and urea as precursors. According to the optical properties of as-prepared CDs, both the excitation and emission spectra of CDs showed quite precise overlapping with the absorption band of curcumin. Thus, CDs can be expected as fluorescent probe for the determination of curcumin based on the IFE behavior. The detection strategy is depicted in Scheme 1. Initially, the free CDs showed strong fluorescence in aqueous solution. Upon adding curcumin, obvious fluorescence quenching can be observed due to the intensive absorption of curcumin to both the excitation and emission light from CDs. On the basis this phenomenon, we established a high sensitive and selective fluorescent method for determination of curcumin in human urine samples.



Scheme 1 Schematic illustration for the sensing of curcumin based on IFE.

2 Experimental

2.1 Chemicals

Curcumin was purchased from Shanghai Chemical Reagent (Shanghai, China). Citric acid and urea were from Sigma–Aldrich Chemical Co.(St.Louis, USA). The solutions of metal cations were prepared from their chlorine salts. A series of Britton–Robinson (BR) buffer solutions (50mM) ($\text{H}_3\text{PO}_4+\text{H}_3\text{BO}_3+\text{HAc}+\text{NaOH}$) were used for the pH adjustment. All the chemicals used were of analytical reagents grade or above without further purification and double-distilled water ($\geq 18.2 \text{ M cm}^{-1}$) from the Millipore Milli-Q system was used throughout.

2.2 Apparatus

All the fluorescence measurements were carried out with a F-4500 fluorescence spectrophotometer (Hitachi, Japan). UV-Vis absorption spectra were performed on a TU-1901 Double beam UV-Vis spectrophotometer (Hitachi, Japan). HPLC were recorded on an Agilent 1200 liquid chromatography system fitted with a analytical column C18 (Agilent SB, 2.1mm \times 50mm \times 1.8 μm). An Agilent 1260 series VWD detector was used for detection at a wavelength of 420 nm. Infrared spectroscopy was carried out using a FTIR-8400S Infrared spectrometer in the form of KBr pellets from 4000 to 500 cm^{-1} . Fluorescence lifetime assays were conducted on a FLS-920 Edinburgh Fluorescence Spectrophotometer (Edinburgh Co., Ltd., England). Transmission electron microscopy (TEM) and high resolution TEM (HR-TEM) images were obtained on a FEI TECNAI G2 F20 U-TWIN transmission electron microscope at an accelerating voltage of 200 kV. The hydrodynamic diameter and zeta potential were measured with a Malvern Zetasizer Nano-ZS90 dynamic light scattering system. A FE20 pH meter (Mettler Toledo, Switzerland) was used to adjust the pH value.

2.3 Preparation of N-doped CDs

Water-soluble N-doped CDs were synthesized via a simple-effective hydrothermal treatment according to a previously published method with slight modifications.^[40] In brief, citric acid (0.576g) and urea (1.0809g) were dissolved to distilled water (15mL) to form a transparent solution. The solution was then heated in a stainless steel autoclave (50mL) at 200 °C for 10 h. After the reaction, the vessel was cooled down naturally to obtain the brown solution, indicating the formation of CDs. Then the crude product was centrifuged at 13000 rpm for 15 min to remove the large or agglomerated solid particles. The aqueous solution of CDs was subject to further purify through a dialysis membrane (MWCO of 1000) in 1 L of Milli-Q water for 2 days. Finally, the resulting aqueous solution was collected from the dialysis membrane and freeze-dried to obtain the N-doped CDs product. The synthetic method can be used to prepare different types of N-doped CDs by tuning the precursors molar ratios as depicted in Fig. S1 † and S2 †.

2.4 Fluorescence measurements

An aliquot of N-doped CDs (90 μL , 1mg/mL) was added to Britton–Robinson(BR) buffer (50mM, pH 7.5, 910 μL). Different volumes of 1×10^{-3} M curcumin stock solution were successively pipetted and mixed thoroughly before determination. In BR buffer, the optimal excitation wavelength of as-prepared CDs was at 360 nm with the maximal emission peaks at the 445 nm for quantitative analysis. The excitation slit width was set as 2.5 nm and the emission slit was 5 nm. All the detections were performed in triplicate.

3 Results and discussion

3.1 Characterization of N-doped CDs

The size distribution and morphology of N-doped CDs were characterized by TEM. As shown in Fig.1A, CDs were well dispersed quasi-spherical nano-dots and meanwhile, the HR-TEM image of N-doped CDs (Fig.1B) showed lattice spacing of 0.23 nm, which agreed with that of in-plane lattice spacing of graphene (100 facet).^[41] Fig. 1C clearly confirmed that CDs obtained here existed as a narrow

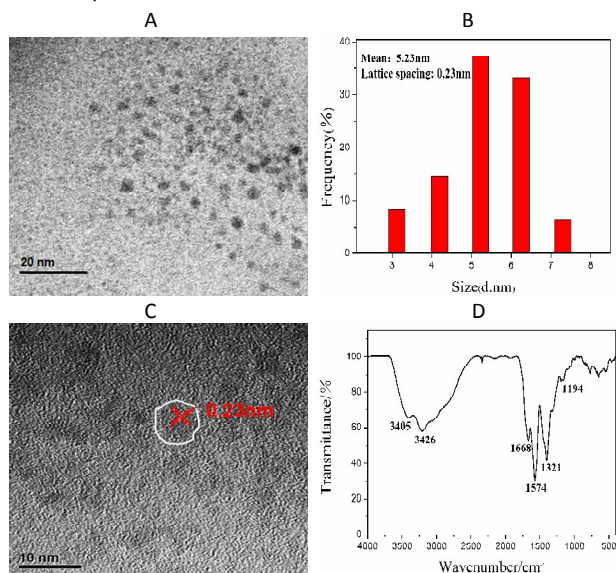


Fig. 1. (A) TEM and (B) HRTEM images of the N-doped CDs; (C) Particle size distribution of the N-doped CDs; (D) FT-IR spectra of the N-doped CDs

distribution with diameters in the range of 4-6 nm and the average is about 5.23 nm (based on statistical analysis of more than 100 dots), in line with the DLS results (Fig. S4 †).

The surface functional groups of the N-doped CDs were characterized by FT-IR spectroscopy (Fig.1D). The peak at 1321 and 1194 cm^{-1} were assigned to the asymmetric and symmetric stretching modes of C–O–C (ether or epoxy).^[42] Simultaneously, the peak at 1574 cm^{-1} was associated with the stretching vibration of C–N, indicating the formation of –CONR.^[43] C=O and C=C stretching vibrations were at 1668 cm^{-1} . In addition, the broad band at 3204–3405 cm^{-1} appeared because of the main absorption band of O–H and N–H stretching vibration.^[44] Similar to earlier reports,^[40] the FT-IR results gave the evidence that the surface of CDs was full of hydrophilic groups: hydroxyl and carboxylic groups, which can improve the hydrophilicity and stability of the CDs in water. In good agreement with FTIR, the zeta potential of the CDs in the aqueous solution was -21.2 mV. The surface of the prepared CDs was covered with carboxyl groups and was negatively charged. Because the same charges repel each other, CDs do not aggregate.

The UV-Vis absorption and photoluminescence (PL) spectra of the as-prepared CDs were also investigated as shown in Fig. 2A. The absorption spectrum of N-doped CDs showed a weak shoulder band at 245 nm and a narrow peak at around 340 nm with a tail extending into the visible range. The two peaks were attributed to $\pi-\pi^*$ transition of the C=C bond and $n-\pi^*$ transition of the C=O bond, respectively. Simultaneously, the maximum excitation and emission wavelengths were located at 360 nm and 445 nm. The image of the

N-doped CDs dispersion under UV light (365 nm) exhibited an obvious blue color (right) while appearing as light brown transparent under daylight (left).

To further explore the optical properties of N-doped CDs, the excitation-wavelength dependent photoluminescence (PL) behavior was shown in Fig.2B. With the increasing excitation wavelength from 310 to 410 nm, the PL first increases and then decreases with a red shift, indicating that PL of N-doped CDs are excitation-dependent. The quantum yield of N-doped CDs was measured to be

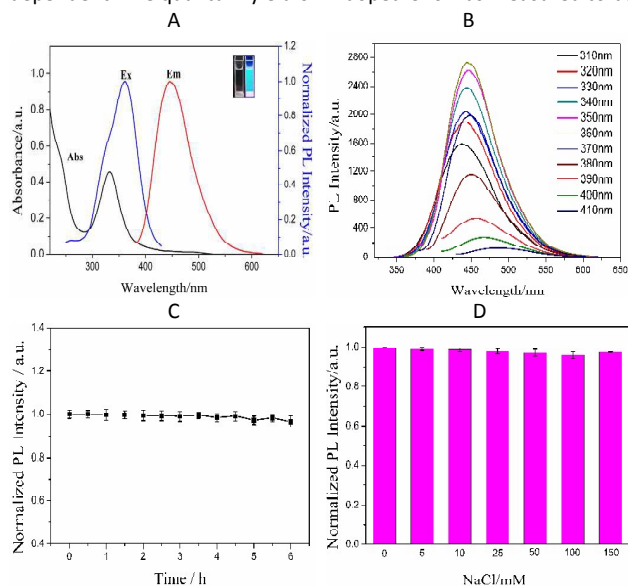


Fig.2. (A) PL spectra and UV-Vis absorption spectra of the N-doped CDs. Inset: Photograph of the obtained CDs under illumination of white light (left) and UV (365 nm) light (right); (B) The PL spectra of N-doped CDs at different excitation wavelengths; (C) PL intensity of N-doped CDs against excitation time; (D) The effect of ionic strength on the N-doped CDs PL intensity.

about 25.4% by using quinine sulfate in 0.1 M sulfuric acid solution (quantum yield 54%) as the standard. By using various molar ratios of citric acid to urea, we found that the molar ratios play a significant role in determining the final quantum yield (QY) (Table S1†). In addition, the CDs exhibited excellent stability. Their PL intensity did not change even under continuous excitation for 6 h (Fig.2C). And although the solution was preserved at 4 °C in the dark for more than three months, there was also no fade significantly in color and PL intensities. In Fig.2D, it was observed that the PL intensity of the N-doped CDs remained constant over a wide concentrations of NaCl solutions (0–150 mM). The results revealed that N-doped CDs possess outstanding stability, tolerance for high ionic strength and photobleaching, which makes them a promising candidate for PL detection.

3.2 IFE between N-doped CDs and curcumin

IFE phenomenon of fluorescence usually occurs between the absorber and fluorophore resulting from the absorption of the excitation and /or emission light by absorbers in the detection

A B

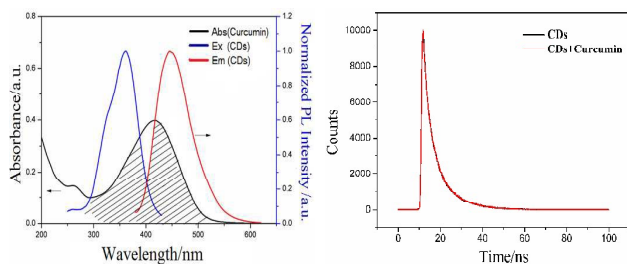


Fig.3. (A) The spectral overlap between the absorption band of the curcumin and the excitation and emission band of the N-doped CDs; (B) The fluorescence decay curve of N-doped CDs in the absence and presence of curcumin upon excitation at 360nm.

system. The effective IFE requires the complementary overlap of the absorber's absorption band with the excitation and/or emission bands of the fluorophore. Therefore, it is important to choose a suitable absorber and fluorophore in the IFE-based fluorescent assays.^[45] As shown in Figure 3A, curcumin possess a wide absorption peak at around from 300 to 550nm. Our as-prepared N-doped CDs were chosen as the fluorophore because both the excitation and emission spectra of CDs showed quite precise overlapping with the absorption band of curcumin. Consequently, as expected from the original design (Scheme 1), curcumin can not only shield the excitation light from CDs but also absorb the emission light of CDs. Naturally, the absorbance enhancement of curcumin could be successfully converted to fluorescence quenching of CDs, which is favorable to enhance the detection sensitivity.

To demonstrate the fluorescence IFE between the N-doped CDs fluorophore and curcumin absorber, the time-resolved fluorescence spectroscopy was executed and the decay spectrum of the N-doped CDs fitted with bi-exponential curve were shown in Fig. 3B. In the absence of curcumin (the black curve), the average lifetime value of N-doped CDs was 7.61ns ($\chi^2=1.082$) with lifetimes of $\tau_1=3.96$ ns (35.34%) and $\tau_2=9.61$ ns (64.66%). In the presence of 30 μ M curcumin (the red curve), the average fluorescence lifetime of the N-doped CDs was 7.62ns ($\chi^2=1.076$) with lifetimes of $\tau_1=4.01$ ns (35.41%) and $\tau_2=9.60$ ns (64.59%). The almost no lifetime change of the N-doped CDs indicated that there is no significant excited-state interaction between N-doped CDs and curcumin, demonstrating that the fluorescence change of N-doped CDs by curcumin resulted from the simple absorption of the excitation and emission light by the absorber.^[46] Also, curcumin is negatively charged, and no electrostatic interaction took place between N-doped CDs and curcumin. This can facilitate our demonstration of the present concept that the fluorescence sensing would be clearly based on the IFE rather than other possible approaches.

3.3 Optimization of experimental conditions

3.3.1 Effect of the N-doped CDs concentration. Fig. 4A showed the effect of the concentration of N-doped CDs on its PL intensity in the presence and absence of curcumin. The PL intensity increased gradually with increasing concentrations of N-doped CDs and reached a maximum, then the PL intensity decreased with further increase of concentrations from the self absorption and inner filter effects of CDs. Upon the addition of curcumin, the PL intensity changes of N-doped CDs showed a tiny concentration-dependent,

and the optimal concentration was about 90mg L⁻¹. Considering the fluorescence background and the sensitivity of the detection, 90 mg L⁻¹ of N-doped CDs was chosen for the following experiment.

3.3.2 Effect of pH. As shown in Fig.4B, deprotonation of carboxylic groups occurred on the surface of the N-doped CDs with the pH increase, and a "protective shell" with negative charge was formed gradually on the surface of CDs with lower non-radiative recombination rate.^[47] This gave rise to the increase of CDs PL intensity. However, when pH was greater than 5.0, the deprotonation of carboxylic groups on the surface of N-doped CDs has been done, and a uniform "protective shell" has been formed. The observed PL intensity almost kept constant. Upon addition of curcumin, the effect of pH on the PL quenching of N-doped CDs was

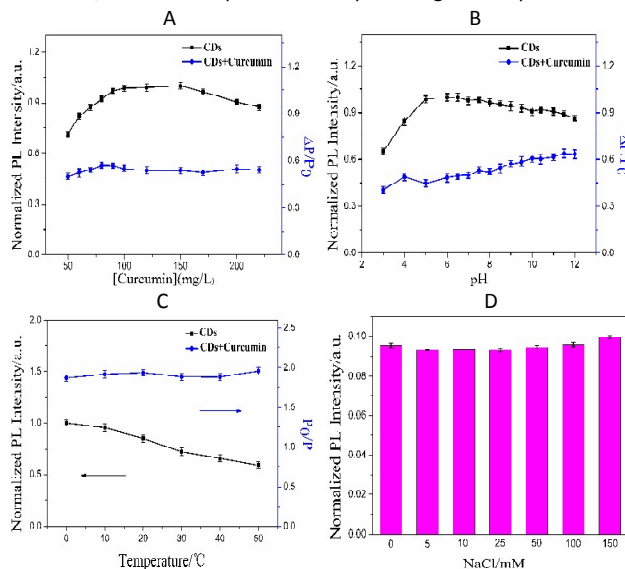


Fig.4. Effect of N-doped CDs concentrations (A) and pH (B) on the PL intensity of CDs (■) and $\Delta P/P_0$ in the presence of curcumin (●). $\Delta P = P_0 - P$, P_0 and P are the PL intensity of N-doped CDs in the absence and presence of curcumin, respectively. (C) Effect of temperature on the PL intensity of N-doped CDs (■) and $\Delta P/P_0$ of the mixture of CDs with curcumin (●). (D) Effect of ionic strength on the PL intensity of N-doped CDs-curcumin.

studied. The quenching efficiency ($\Delta P/P_0$) of the N-doped CDs gradually increased in the pH range from 5.0 to 12.0. This phenomenon accorded well with the absorbance characteristic of curcumin, namely, the absorption slowly enhanced with a red shift from 420 nm in acid media to 463 nm in basic media (Fig.S5†).^[48] At higher pH, curcumin absorbed the excitation and emission light of CDs more intensively, and the emission intensity decreased correspondingly. The result also provided the further evidence that the PL intensity of N-doped CDs was decreased by curcumin based on the IFE. Whereas, curcumin possesses highly stable properties under acidic and neutral conditions.^[49] Considering the normal physiological pH values and the stability of curcumin, pH=7.5 was chosen for all subsequent detection assays.

3.3.3 Effect of temperature and ionic strength. Temperature and ionic strength play pivotal roles in the PL intensity of CDs-curcumin system. As revealed in Fig.4C, the N-doped CDs showed the temperature-dependent PL intensity in the absence of curcumin.

However, the temperature had very little effect on the PL intensity in the presence of curcumin. The experiments were performed at room temperature ($20\pm 3^\circ\text{C}$) for the convenience purpose. Additionally, using NaCl as the ionic strength regulator, the PL intensity of CDs–curcumin system kept constant with varied concentrations of NaCl in the aqueous solution (Fig.4D). On this basis, the possibility of PL quenching via the electrostatic

interaction between N-doped CDs and curcumin was further excluded.^[50]

3.4 Detection Selectivity

Selectivity is an important parameter to evaluate the anti-interference performance of the sensing system. The PL response

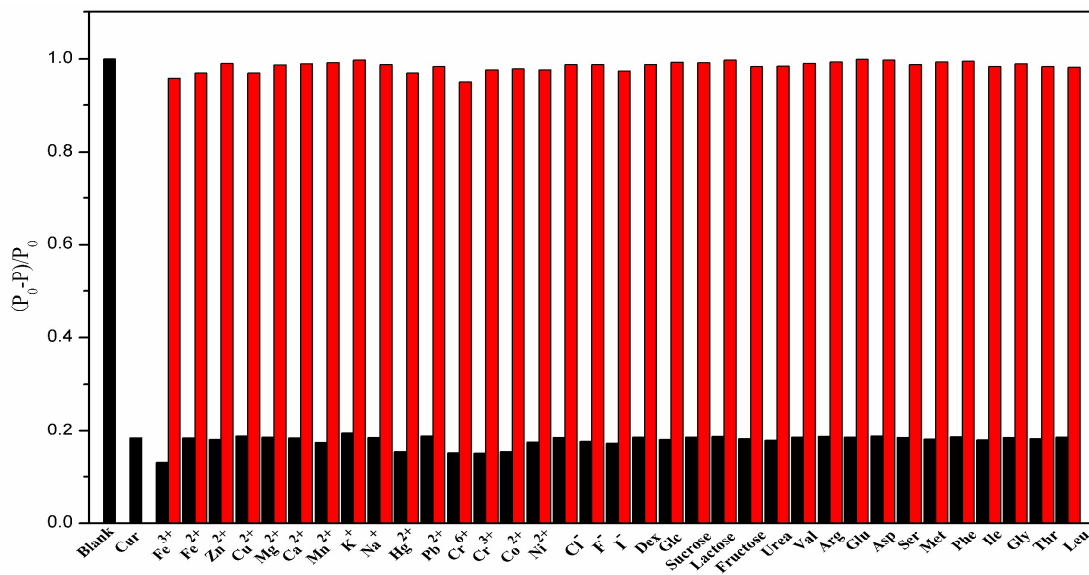


Fig.5. Selectivity of the sensing method against other ions and compounds. Concentrations of curcumin and other ions and compounds were $30\mu\text{M}$ and 3mM , respectively. Red bars represent the responses of the sensing system challenged with a specific ion or compound. Black bars show the responses of the sensing system in the presence of $30\mu\text{M}$ curcumin and 3mM corresponding ions or compounds.

when the sensing system was challenged with other potential interfering substances, including some common metal ions (Fe^{3+} , Fe^{2+} , Zn^{2+} , Cu^{2+} , Mg^{2+} , Ca^{2+} , Mn^{2+} , K^+ , Na^+ , Hg^{2+} , Pb^{2+} , Cr^{6+} , Cr^{3+} , Co^{2+} , Ni^{2+}), anions (Cl^- , I^- , F^- , Br^-), small organic molecules (glucose, sucrose, fructose, lactose) and amino acid (L-valine, L-arginine, L-Glutamate, L-Asparagine, L-Serine, L-Methionine, L-Phenylalanine, L-histidine, L-lysine, L-Glycine, L-threonine) which possibly existed in the real samples was monitored. As shown in Fig.5 (red histograms), $30\mu\text{M}$ curcumin produced a more significant fluorescence quenching compared with that caused by other analytes mentioned above at ultrahigh concentrations (concentration is 100-fold of curcumin). Fig.5 (black histograms) also revealed that the coexistence of curcumin and other ions and compounds did not affect detection by the N-doped CDs probe. These results demonstrated that the N-doped CDs shows excellent selectivity toward curcumin over other common ions and compounds.

3.5 Analytical merits of curcumin

The PL intensity quenching of the N-doped CDs at various concentration of curcumin were displayed in Fig. 6A. Fig. 6B showed the Stern-Volmer plot of N-doped CDs with increasing concentration of curcumin (P_0/P against concentration of curcumin). The quenching efficiency was fitted by the Stern-Volmer equation, $P_0/P = 1 + K_{sv}[Q]$, where K_{sv} is the Stern-Volmer

quenching constant and $[Q]$ is the curcumin concentration. The K_{sv} was calculated to be 0.10215 L/mol with a correlation coefficient r^2 of 0.998. The P_0/P curve was linearly related to the concentration of curcumin in the range of 2.0×10^{-7} – $1.0\times 10^{-5}\text{ mol/L}$, indicating their excellent sensing properties in the detection of trace curcumin. And the relative standard deviation (RSD) of the proposed method was 3.17% ($n=11$). The limit of detection (LOD) was calculated by taking

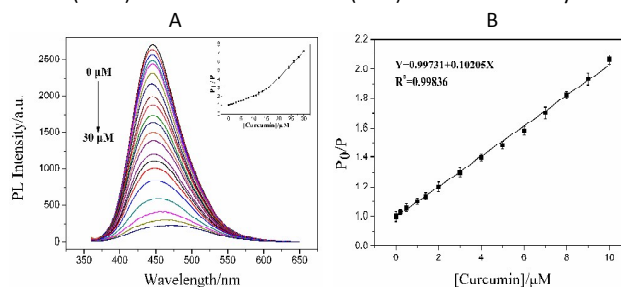


Fig.6 (A) PL spectra of N-doped CDs in the presence of curcumin at various concentrations at pH 7.5. Amounts of curcumin were 0, 0.2, 0.5, 1.0, 1.4, 2.0, 3.0, 4.0, 5.0, 6.0, 7.0, 8.0, 9.0, 10.0, 11.0, 12.0, 14.0, 15.0, 16.0, 20.0, 24.0, 26.0, 28.0 and $30.0\mu\text{M}$ from top to bottom, respectively. Inset: The relationship between the concentration of curcumin and P_0/P ; (B): Linear calibration plot for curcumin detection.

the PL intensity equal to 3 times the standard deviation of the intensity at the blank (n=10) divided by the slope of the calibration graph. The LOD of the proposed method was 8.48×10^{-8} mol/L. The LOD was much lower than some other reported values (Table S2[†]). It was clearly demonstrated the present method with high sensitivity.

3.6 Analytical application of curcumin

For testing the practicality of this developed approach, recovery experiments were performed in human urine samples obtained from the volunteer students (Table 1). As listed, the recoveries of curcumin were in range of 95.71-103.80%, revealing satisfactory consistencies between the actual and the measured concentrations. Also, to check the accuracy of the method, a high performance liquid chromatography (HPLC) was used to measure the curcumin in the human urine samples (Fig.S6[†]).^[51] As shown in Table 1, there was a good agreement between the results obtained by our developed method and by HPLC, indicating that the proposed

method may broaden ways for practical detection of curcumin in real samples.

4 Conclusions

In summary, we have developed and validated a simple, convenient, high sensitive and selective method for curcumin analysis using N-doped CDs as a fluorescent probe based on the inner filter effect. Curcumin can not only hide the excitation light of CDs but also absorb the emission light from CDs, and naturally, the PL intensity of the N-doped CDs was quenched obviously with increasing curcumin concentration. This method has been applied towards the detection of curcumin contents in human urine samples with satisfactory results. To the best of our knowledge, this is the first demonstration of a CDs-based nanosensor for curcumin via fluorescent inner filter effect. We believed that this method might pave a new way for the further exploration and practical application in analytical detection and chemical sensing area.

Table 1 Determination of curcumin contents in human urine samples.

Urine Sample	Added (μM)	Found (μM)		Recovery(%)		RSD(n=6) of Proposed method (%)
		Proposed method	HPLC	Proposed method	HPLC	
1	0.70	0.67	0.71	95.71	101.43	2.17
	5.00	5.19	5.13	103.80	102.60	0.79
2	0.70	0.71	0.72	101.43	102.86	2.94
	5.00	4.89	5.19	97.72	103.80	3.25
3	0.70	0.72	0.73	102.86	104.28	1.78
	5.00	5.11	5.24	102.20	104.80	1.44

Acknowledgements

Financial supports from the National Natural Science Foundation of China (No. 21475080 and 21575084), Shanxi Province Hundred Talents Project, Shanxi Scholarship Council of China (No.2013 - key 1).

Notes and references

- 1 T.H. Cooper, G. Clark, J. Guzinski, *J. Am. Chem. Soc.*, 1994, **547**, 231-236.
- 2 P.Basnet, N.Skalko-Basnet, *Molecules*, 2011,**16**, 4567-4598.
- 3 S. Bengmark, J.Parenter, *Enterol. Nutr.*, 2006, **30**, 45-51.
- 4 R. A. Sharma, S. A. Euden, S. L. Platton, D. N. Cooke, A. Shafayat, H. R. Hewitt, *Clin. Cancer. Res*, 2004, **10**, 6847-6854.
- 5 R. A. Sharma, A. J. Gescher, W. P. Steward, *Eur. J. Cancer*, 2005, **41**, 1955-1968.H. Zhou, C.S. Beevers, S. Huang, *Curr. Drug Targets*, 2011, **12**, 332-347.
- 6 H. Zhou, C.S. Beevers, S. Huang, *Curr. Drug Targets*, 2011, **12**, 332-347.
- 7 G.K. Ziyatdinova, A.M. Nizamova, H.C. Budnikov, *J. Anal. Chem.*, 2012, **67**, 591-594.
- 8 W.H. Chan, H.Y. Wu, W.H. Chang, *Food Chem. Toxicol.*, 2006, **44**, 1362-1371.
- 9 F. Wang, W. Huang, Y.W. Wang, *J. Lumin.*, 2008, **128**, 110-116.

- 10 F. Wang, W. Huang, *J. Pharm. Biomed. Anal.*, 2007, **43**, 393-398.
- 11 A. Navas Diad, M. C. Ramos Peinado. *J. Agric. Food Chem.*, 1992, **40**, 56-59.
- 12 B. Tang, L. Ma, H.Y. Wang, G.Y. Zhang, *J. Agric. Food Chem.*, 2002, **50**, 1355-1361.
- 13 G. K. Ziyatdinova, A. M. Nizamova, H. C. Budnikov, *J. Anal. Chem.*, 2012, **67**, 591-594.
- 14 M. Lechtenberg, B. Quandt, A. Nahrstedt, *Phytochem. Anal.*, 2004, **15**, 152-158.
- 15 M. Rahimi, P. Hashemi, F. Nazari, *Anal. Chim. Acta*, 2014, **826**, 35-42.
- 16 J. Li, Y.Y. Jiang, J. Wen, G.R. Fan, Y.T. Wu, C. Zhang, *Biomed. Chromatogr.*, 2009, **23**, 1201-1207.
- 17 J. H. Lee, M.G. Choung, *Food Chem.*, 2011, **124**, 1217-1222.
- 18 D. D. Heath, M. A. Pruitt, D. E. Brenner, C. L. Rock, *J. Chromatogr. B*, 2003,**783**, 287-295.
- 19 Z.G. Chen, L. Zhu, T.H. Song, J.H. Chen, Z.M. Guo. *Spectrochim. Acta, Part A.*, 2009, **72**, 518-522.
- 20 X.J. Zhao, F.X. Lia, Q.Y. Zhang, Z.B. Li, Y.H. Zhou, J. Yang, C. Dong, J.P. Wang, S.M. Shuang, *RSC Adv.*, 2015, **5**, 21504-21510.
- 21 S. K. Bhunia, A. Saha, A. R. Maity, S.C. Ray, N.R.Jana, *Sci. Rep.*, 2013, **3**, 1473-1478.
- 22 H. Li, Z. Kang, Y. Liu, S.T. Lee, *J. Mater. Chem.*, 2012, **22**, 24230-24253.

Journal Name ARTICLE

- 23 J. Shen, Y. Zhu, X. Yang, C. Li, *Chem. Commun.*, 2012, **48**, 3686-3699.
- 24 Y.F. Wang, A.G. Hu, *J. Mater. Chem. C*, 2014, **2**, 6921-6939.
- 25 W.P. Wang, Y.C. Lu, H. Huang, J.J. Feng, J.R. Chen, A.J. Wang, *Analyst*, 2014, **139**, 1692-1696.
- 26 W.P. Wang, Y.C. Lu, H. Huang, A.J. Wang, J.R. Chen, J.J. Feng, *Biosensors and Bioelectronics*, 2015, **64**, 517-522.
- 27 X.H. Gao, Y.Z. Lu, R.Z. Zhang, S.J. He, J. Ju, M.M. Liu, L. Li, W.Chen, *J. Mater. Chem. C*, 2015, **3**, 2302-2309.
- 28 J. Ju, W.Chen, *Biosensors and Bioelectronics*, 2014, **58**, 219-225.
- 29 Y. Dong, H. Pang, H.B. Yang, C.Guo, J. Shao, Y. Chi, C.M. Li, T. Yu, *Angew.Chem. Int.Ed.*, 2013, **52**, 7800-7804.
- 30 P. Ayala, R. Arenal, A. Loiseau, A. Rubio, T. Pichler, *Rev.Mod. Phys.*, 2010, **82**, 1843-1885.
- 31 M. J. Krysmann, A. Kellarakis, P. Dallas, E. P. Giannelis, *J. Am. Chem. Soc.*, 2012, **134**, 747-750.
- 32 J. Ju, R.Z. Zhang, S.J. He, W.Chen, *RSC Adv.*, 2014, **4**, 52583-52589.
- 33 J. Ju, W.Chen, *Anal. Chem.*, 2015, **87**, 1903-1910.
- 34 R.Z. Zhang, W. Chen, *Biosensors and Bioelectronics*, 2014, **55**, 83-90.
- 35 A. Zhao, C. Zhao, M. Li, J. Ren, X. Qu, *Anal.Chim. Acta*, 2014, **809**, 128-133.
- 36 Q. Wang, X. Liu, L.C. Zhang, Y. Lv, *Analyst*, 2012, **137**, 5392-5397.
- 37 N. Shao, Y. Zhang, S. M. Cheung, R. H. Yang, W. H. Chan, T. Mo, K. A. Li, F. Liu, *Anal. Chem.*, 2005, **77**, 7294-7303.
- 38 L. Shang, S. J. Dong, *Anal. Chem.*, 2009, **81**, 1465-1470.
- 39 M. Zheng, Z.G. Xie, D. Qu, D. Li, P. Du, X.B. Jing, Z.C. Sun, *Appl. Mater. Interfaces*, 2013, **5**, 13242-13247.
- 40 B.B. Wang, Y.F. Wang, H. Wu, X.J. Song, X. Guo, D.M. Zhang, X.J. Ma, M.Q. Tan, *RSC Adv.*, 2014, **4**, 49960-49963.
- 41 Y.Q. Dong, H.C. Pang, H.B. Yang, C.X. Guo, J.W. Shao, Y.W. Chi, C.M. Li, Ti. Yu, *Angew. Chem. Int. Ed.*, 2013, **52**, 7800-7804.
- 42 Y. Liu, N. Xiao, N. Gong, H. Wang, X. Shi, W. Gu, L. Ye, *Carbon*, 2014, **68**, 258-264.
- 43 X. Zhai, P. Zhang, C. Liu, T. Bai, W. Li, L. Dai, W. Liu, *Chem. Commun.*, 2012, **48**, 7955-7957.
- 44 J. Jiang, Y. He, S.Y. Li, H. Cui, *Chem. Commun.*, 2012, **48**, 9634-9636.
- 45 L. Shang, S.J. Dong, *Anal. Chem.*, 2009, **81**, 1465-1470.
- 46 D.W. Zhang, Z.Y. Dong, X.Z. Jiang, M.Y. Feng, W. Li, G.H. Gao, *Anal. Methods*, 2013, **5**, 1669-1675.
- 47 W. Kong, H. Wu, Z. Ye, R. Li, T. Xu, B. Zhang, *J. Lumin.*, 2014, **148**, 238-242.
- 48 Q. Zhao, D.X. Kong, H.Y. Zhang, *Nat. Prod. Commun.*, 2008, **3**, 229-232.
- 49 Y.J. Wang, M.H. Pan, A.L. Cheng, L.I. Lin, Y.S. Ho, C.Y. Hsieh, J.K. Lin, *J. Pharm. Biomed. Anal.*, 1997, **15**, 1867-1876.
- 50 P.T. Burks, A.D. Ostrowski, A.A. Mikhailovsky, E.M. Chan, P.S. Wagenknecht, P.C. Ford, *J. Am. Chem. Soc.*, 2012, **134**, 13266-13275.
- 51 G. K. Jayaprakasha, L. J. Rao, K. K. Sakariah, *J. Agric. Food Chem.*, 2002, **50**, 3668-3672.